euspen's 20th International Conference & Exhibition, Geneva, CH, June 2020
www.euspen.eu

Optimized design of a novel xy parallel micro/nano positioning stage with a concave-shape bridge amplifier

Xingjian Jiang [1,2], Xiaomei Chen[1], Weihu Zhou[1,2]

[1]*Institute of Microelectronics of the Chinese Academy of Sciences*
[2]*University of Chinese Academy of Sciences*

chenxiaomei@ime.ac.cn

Abstract
This paper presents the design, analysis, optimization and verification of a novel two degree-of-freedom (2-DOF) micro/nano positioning stage actuated by piezoelectric (PZT) actuators. This micro/nano positioning stage can be used to establish an atomic-force-microscope (AFM) measurement system. A kind of stacked parallel structure is adopted in order to realize a compact and relative symmetrical design. A novel concave-shape bridge amplifier is proposed and utilized in the positioning stage to amplify the stroke of PZT actuators. The amplifier can realize high lateral stiffness, which is an important factor in protecting PZT actuators. The amplifiers are integrated into decoupling mechanisms isolating the top plate motion in two directions. Finite-element analysis (FEA) and Multi-objective genetic algorithm (MOGA) are conducted on the proposed model to optimize and decide the value of the main design variables. The improved performances compared with the initial design are verified by FEA methodology. Results show that the stage can implement 2-DOF decoupled motion in a workspace of 100×100 μm^2 with a mechanisim system surface of 100×100mm^2.

Micro/nano-positioning, Flexure hinges, Finite-element analysis, Mechanism design, Concave-shape bridge amplifier

1. Introduction

Micro/nano positioning is an important technology widely applied in the field of micro-electro-mechanical systems (MEMS). Micro/nano positioning stages are broadly used in precision applications, such as biological micromanipulation, optical fiber alignment, nano-imprint lithography, scanning probe microscopes(SPM), micro/nano assembly and etc[1-2].

Atomic force microscopy (AFM) is a kind of SPM, with demonstrated resolution on the order of fractions of a nanometer. In general, the measurement object of AFM should be carried by a nanopositioning stage to guarantee the precision. Therefore, a novel XY nanopositioning stage is designed, it can carry the sample and control the precise displacement of the sample to realize two-dimensional scanning.

Before design, the desired performance should be clear. In this AFM measument system, the workspace demand is 100×100 μm^2 at least. Besides, the demand towards positioning accuracy is 100 nm. In terms of the load limit of the stage, it is expected to be more than 500g. In addition, for operating in a limited space, the XY stage is expected to possess a compact structure. Thus, the compactness of the XY stage is an important design criterion. The compactness index can be defined as the ratio between the workspace and device area of the XY stage[3]. A larger compactness index implies that the stage can be fabricated with a smaller footprint size for achieving a defined workspace size.

In practice, XY precision positioning stages have been intensively studied owing to their various applications[3-4]. They can be classified into two types on the basis of conventional mechanical transmission mechanism and flexure-based compliant mechanism. Flexure hinge can eliminate important factors including friction and backlash, which is benefitial to guarantee the positioning accuracy. In addition, the structure of flexure is simple and easy to fabricate. On the contrary, traditional transmission mechanism can not meet the demand of precison[5-6]. Therefore, flexure-based compliant mechanism is suitable for the micro/nano positioning platform of this measurement system.

The two degree-of-freedom (2-DOF) compliant mechanism system can be classified into two types in terms of serial-kinematic structure and parallel-kinematic structure. Parallel-kinematic mechanism has various advantages, such as large stiffness, no cumulative error and the fast response. It is more suitable than the serial-kinematic mechanism to cater for the requirement of precision motion output[7-8].

However, it is still challenging to devise a compact parallel-kinematic XY stage with larger travel stroke driven by piezoelectric actuators[9]. In the category of parallel flexible structure, single-layer structure, stacked structure and 3D overall structure are three main types. It is difficult to make full use of vertical space adopting single-layer structure, which means this structure is unlikely as compact as demanded. 3D overall parallel structure as an alternative needs to be fabricated by 3D printing technology. But the processing precision is not high enough with current technical level[9-10]. Through overall consideration, stacked structure is adopted.

In the literature, parallel-kinematic XY stages with stacked structure have been developed[11-14]. However, the existing XY stages exhibit large crosstalk between the two working axes[9].

To this end, a new stack-type XY parallel nanopositioning stage is devised to realize a more compact structure with decoupled

motion. Analytical modeling, optimization, simulation testing are conducted to impove and verify the stage performance. The remaining parts of the paper are organized as follows. The mechanism design of the new XY stage is presented in Section 2 . The optimization design is performed in Section 3 , where the structure improvement and FEA simulation are carried out. Section 4 shows the simulation verification results and comparison with existing stages. Section 5 concludes this paper.

2. Mechanical structure

The structure of the stacked parallel stage can be devided into four main parts including actuator, amplifier, guiding structure and decoupling structure. In this section, the mechanical design of the XY stage is presented.

2.1. Displacement amplifier design

Piezoelectric actuators (PZT) are adopted as the actuators of the micro/nano positioning stage. However, the stroke of a PZT is relatively small. In order to achieve a large workspace and a compact dimension, displacement amplifiers are needed. In general, displacement amplifiers can be classified into lever-type and bridge-type mechanisms according to different amplifying principles.

Compared with the lever-type amplifier, bridge-type amplifier can offer a larger amplification ratio with a similar size. This means that a more compact structure can be obtained by adopting the bridgetype amplifier[9]. Therefore, the bridge-type displacement amplifier is used in this work.

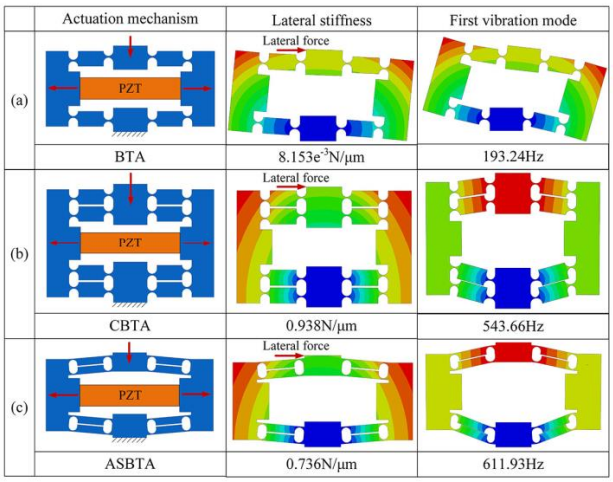

Figure 1. Comparison of different amplifiers: (a) BTA (b) CBTA (c) ASBTA

Many existing stages adopt conventional bridge type amplifier (BTA) as the PZT actuation mechanism as shown in figure 1(a) [15]. However, the relatively low lateral stiffness of conventional BTA usually results in undesirable lateral motion when bearing external load, which may damage PZT actuators, and there is an undesired first order vibration mode with a low resonant frequency. To overcome the above shortcomings, compound bridge type amplifier mechanism (CBTA) is proposed[16], as shown in figure 1(b), which significantly increases the lateral stiffness and the first order natural frequency, but the extra bridges with conventional flexure hinges usually result in large dimension size, which enlarges the size of actuation mechanism. Alternatively, a kind of arch-shape bridge type amplifier (ASBTA) with compact structure and large lateral stiffness is proposed, as depicted in figure 1(c). Compared to CBTA in figure 1(b), the ASBTA not only has the same level of lateral stiffness and compact size, but also with a higher first order vibration frequency[17].

However, the maximum dimension in the output direction of the ASBTA will increase with the increase of the angle between the bridge arm and the horizontal line, which will lead to the expansion of the overall size of the platform, and require setting many size parameters in other parts of the platform. It can be seen that the ASBTA is not conducive to realize a compact design and makes trouble in parametric modelling process. Therefore, a new concave-shape bridge amplifier as shown in figure 2 is proposed and applied in the platform of this work, which avoids the problems caused by the ASBTA while ensuring that other performance can also meet the requirements.

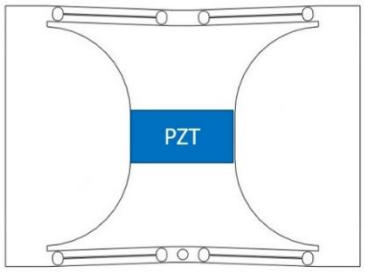

Figure 2. Concave-shape bridge amplifier

2.2. Guiding mechanism and decoupling mechanism

Due to the use of displacement amplifier, the decentration of its mounting hole should be considered. It can induce an unbalanced movement while the stage is in operation. Thus, four leaf flexures are added on both ends of the bridge-type amplifier to serve as the guiding mechanism to ensure the motion platform moving in one axis and eliminate the unbalance of movement[9].

Besides, in order to simplify the control design process, decoupling mechanism is needed. Because parallel-kinematic mechanism output motions in different axes are usually coupled together if there is no decoupling part. In fact, there are many parallel stages by applying decoupled mechanisms in the literature, like[9], which is adopted in this work.

The combined structure of amplifying, guiding and decoupling parts is illustrated in figure 3 . This figure shows one of the two layers of the stage.

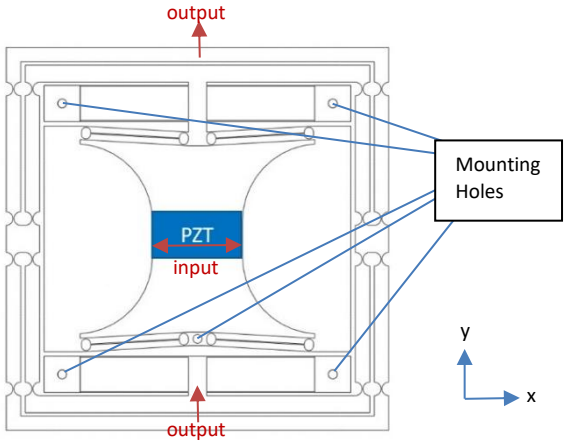

Figure 3. The combination of amplifying, guiding and decoupling parts

2.3. Stage assembly

In this work, the stacked structure is adopted to realize a compact design. Instead of extending the planar area, it makes full use of the vertical space to place the components. figure 4 shows the CAD model of the designed XY stage. Each axis is realized by one layer of the structure as shown in figure 3 . The bottom-up assembly sequence is: base of the whole stage, X-axis mechanism, base of Y-axis mechanism, Y-axis mechanism and finally the top output platform. Besides, there are two connectors for each layer, which are connected to the top platform. When the XY stage is in operation, the output

displacement from each axis will be transmitted through the connectors to the top output platform. The connectors are also used as the sensing targets for the two displacement sensors.

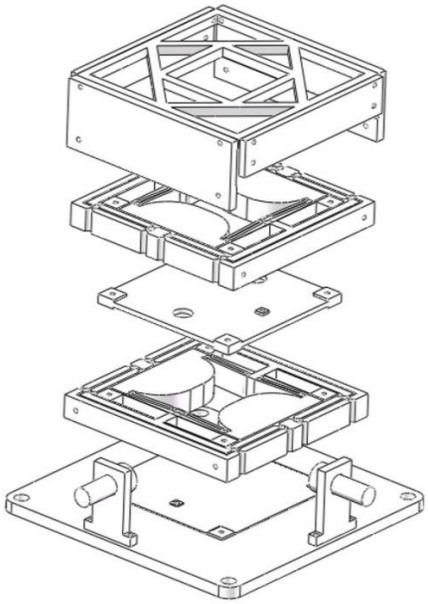

Figure 4. CAD model of the designed XY stage (Exploded view)

3. Optimization and FEA simulation

In this section, a design improvement is proposed, which reduces the thickness and mass of the stage. Afterwards ,the optimal design of the XY stage parameters is conducted and FEA simulation is carried out.

3.1. Design improvement

A CAD model of the improved XY stage is shown in figure 5 . This design improvement reduces the number of moving parts as well as the difficulty of assembly. Besides, the thickness and mass of the stage are both reduced.

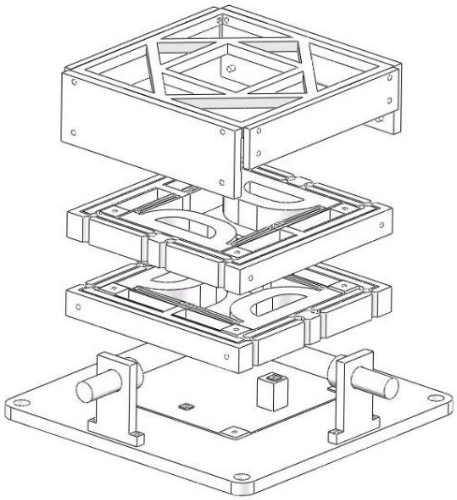

Figure 5. CAD model of the improved XY stage (Exploded view)

3.2. Design optimization method

In mechanical design, the optimization is usually performed by a well-derived mathematical model of the structure. To obtain an accurate result, the model needs to incorporate different factors which affect the result. However, the derivation of an accurate model is difficult for some cases, especially for a complex structure with diverse parameters.

With fine meshing of the solid model and reasonable settings, FEA has the capability to provide reliable results instead of the complex mathematical model[9]. By using the built-in optimization module in FEA software (ANSYS Workbench), only the solid model, objectives and constraints need to be defined. Moreover, it provides various advanced optimization algorithms. In this case, the multi-objective genetic algorithm (MOGA) is used owing to its efficiency to find the global optima. It is a variant of the popular non-dominated sorting genetic algorithm based on the concept of controlled elitism. It supports multiple objectives and constraints and aims at finding the global optima rapidly.

3.3. Optimization elements

Optimization targets, design variables and constaint are three key elements of optimal design. They are supposed to be determined before optimization setup.

In order to characterize the compactness of the proposed design, the compactness index is adopted[3], which is calculated by:

$$C = W/S \tag{1}$$

where, C is compactness index, W is workspace and S is stage covering area.

When the general design scheme is determined, the area occupied by the platform is basically determined, so the working space becomes the most important factor affecting the compactness of the platform. The expression of workspace is:

$$W = X_{max} \times Y_{max} \tag{2}$$

where, W is workspace, X_{max} is X-axis maximum output displacement and Y_{max} is Y-axis maximum output displacement.

The maximum output displacement can be expressed as:

$$O_{max} = I_{max} \times A \tag{3}$$

where, O_{max} is the maximum output displacement, I_{max} is the maximum input stroke and A is amplification ratio.

When the PZT is determined, the maximum output displacement is determined by the input stiffness and amplification ratio of the structure. In fact, the amplification ratio can be calculated from the given input displacement and corresponding output displacement. Thus, the output disacement under the given input is selected as an optimization objective. It can be seen that the optimization objective is related to the part of the amplifier, so two size parameters of the amplifier part in figure 6 are set as the design variables. To facilitate practical manufacturing, the parameter values are truncated to keep one decimal. The optimization elements are shown in detail by table 2.

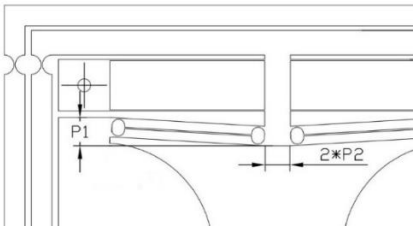

Figure 6. Two selected parameters of the structure

3.4. Optimization setup and results

Al-7075 is selected as the material of the XY stage because of its high stiffness and low density. Especially, its low density can reduce the effect of the vertical loading, which is induced by the stacked design. Table 1 lists the main mechanical properties of Al-7075, which are used in the FEA simulation. Table 2 indicates the elements and results of the optimization. Table 3 shows the promotion of performance throughout structure optimization and improvement.

Table 1 Mechanical properties of Al-7075 material.

Property	Value
Density (kg m^{-3})	2810
Young's modulus (GPa)	71.7
Poisson's ratio	0.33
Tensile yield strength (MPa)	503

Table 2 Elements and results of the optimization.

Item	Constraint	Objective	Result
P1 (mm)	[3.9,4.7]	-	4.6
P2 (mm)	[1.7,2.1]	-	1.8
Output DISP (μm)	-	maximum	118
Input Stiffness(N/m)	< 2×10^7	-	1.5×10^7

Table 3 The promotion of performance throughout structure optimization and improvement.

Objective	Former	Later	Proportion
X output (μm)	102	118	Increased by 16%
Y output (μm)	102	118	Increased by 16%
Mass (g)	385	327	Reduced by 15%
Thickness (mm)	32	28	Reduced by 12.5%

4. Verification results

After optimization several simulation tests should be done in order to verify the final design. It is a necessary step before practical fabrication of a prototype. In this work, maximum stress, life, cross-axis error and four vibration modes are verified.

Equivalent stress simulation result is shown in in figure 7 . It can be noticed that the maximum equivalent stress value is 5.2×10^7Pa. It is less than the allowable stress of the material, which is calculated by :

$$\sigma_{allow} = \sigma_m/s_f = 201.2\text{MPa} \quad (\sigma_m = 503\text{MPa}, s_f = 2.5) \qquad (4)$$

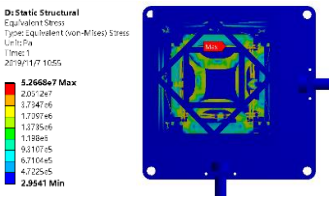

Figure 7. Equivalent stress simulation

Applying fatigue tool of ANSYS workbence, it is proved that the life of the proposed flexure structure is more than 10 million cycles of working loads. So, the life of the stage is qualified.

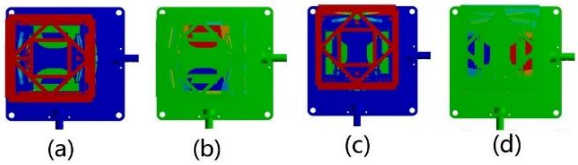

Figure 8. The FEA results of (a) X output (b) Y parasitic (c)Y output (d) X parasitic displacement.

Cross coupling is the key performance of the 2-DOF micro-positioning stage. The FEA results of the output displacement in working direction are shown in figure 8 (a), (c), respectively. The FEA results of the parasitic displacement in non-working direction are shown in figure 8 (b), (d), respectively. Cross-axis error is calculated to be less than 0.6%. The order of magnitude of the value shows the fine performance of motion decoulpers.

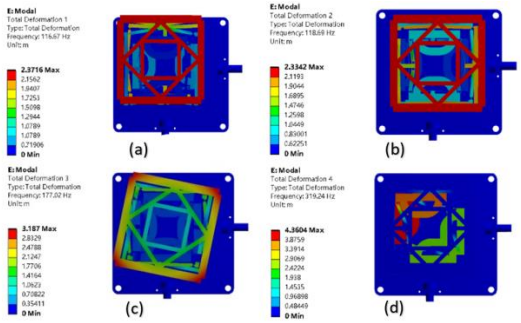

Figure 9. The natural frequency of (a) the first, (b) the second, (c) the third and (d) the fourth mode shape.

The mode shapes of the first four order natural frequencies are shown in figure 9 (a), (b), (c), and (d), respectively. It is found that the first two order natural frequencies are 116.67 Hz and 118.69 Hz with the expected mode shapes along X-axis and Y-axis, respectively. It indicates that the two output axes have a similar dynamic behavior and performance. Moreover, the third order natural frequency occurs around 177.02 Hz, which is larger than the first two order natural frequencies. That is, the parasitic modes occur at frequencies higher than those of the two desired working modes. Hence, the XY stage has a stable translational output motion in X and Y axes.

5. Conclusion

In summary, this work proposes a parallel flexible stage with concave-shape bridge amplifier structure. Through reasonable design, structural improvement and parameter optimization, the stage has achieved relatively ideal displacement outputs, so it has achieved a good compactness and cross-axis error level. Through further simulation analysis, it is verified that the life, maximum stress and mode shapes of the platform meet the requirements. That is, the rationality of the design scheme is verified in various aspects. This work is a successful attempt. Some key technologies of the micro/nano positioning stage have been researched, and the expected results have been achieved, which provides a good foundation for further research on nanopositioning technology.

References

[1] Chen X and Li Y 2017 *Micromachines* **8** 1–13
[2] Polit S and Dong J 2011 *IEEE/ASME Trans. Mechatronics* **16** 724–733
[3] Xu Q 2012 *IEEE Trans. Rob.* **28** 478–491
[4] Hao G and Yu J 2016 *Mech. Mach. Theory* **102** 179–195
[5] Yue Y, Gao F, Zhao X and Ge Q J 2010 *Mech. Mach. Theory* **45** 756–771
[6] Berselli G, Guerra A, Vassura G and Andrisano A O 2014 *IEEE/ASME Trans. Mechatron.* **19** 1882–95
[7] Li Y, Huang J and Tang H 2012 *IEEE Trans. Auto. Sci. & Eng* **9** 538-553
[8] Du Y, Li T, Jiang Y and Wang H 2016 *Advances in Mechanical Engineering* **8** 1-13
[9] Wu Z and Xu Q 2018 *Mechanism and Machine Theory* **126** 171-188
[10] Zhang Z, Yang X and Yan P 2019 *Mechanical Systems and Signal Processing* **117** 757-770
[11] Li Y, Xu Q 2011 *IEEE Trans. Ind. Electron* **58** 3601–15
[12] Xu Q 2014 *IEEE Trans. Ind. Electron* **61** 893–903
[13] Clark L, Shirinzadeh B, Zhong Y, Tian Y and Zhang D 2016 *Mech. Mach. Theory* **105** 129–144
[14] Wan S and Xu Q 2016 *Mech. Mach. Theory* **95** 125–139
[15] Liu Pand Yan P 2016 *Mech. Mach. Theory* **99** 176-188
[16] Li Y and Xu Q 2009 *IEEE Trans. Robot* **25** 645-657
[17] Wang F 2018 *IEEE Transactions on Industrial Electronics* 1-1